SoundSelect Array System

A Directional Hearing Aid Capstone Project

EECE4792

Electrical and Computer Engineering Capstone

Professor Charles DiMarzio

Tim Deignan
Keenan Hye
Mark Long
Steve Muscari
Jack Tarricone

1 Contents

2 Abstract

The SoundSelect Array System team has designed and implemented a system capable of isolating speech emanating from a specific direction in a room and relaying that speech to a user. The system can be virtually steered towards the speech source of interest, thereby reducing the relative gain of other sound sources. While the system has a wide variety of applications, including the fields of audio conferencing and television broadcasting, herein the team will focus on the use of the system as an aid for the hearing impaired. Hearing aid systems currently on the market are also designed to improve speech intelligibility. However, they generally amplify sounds from all directions indiscriminately. This works well in the near-field since the closest and therefore loudest speech source is typically the desired speech source. In the far-field, the lack of microphone directionality and reduced signal to noise ratio make it difficult to understand a particular individual. The SoundSelect Array System solves this problem by focusing a microphone array on a specific target.

To use the SoundSelect Array System, an individual operates a control station connected to a single microphone array. Audio signals from each microphone in the array are sent to the control station for digital signal processing. Using a technique known as delay and sum beamforming, the signals from the individual microphones are delayed relative to the angle of arrival of the target sound and summed back together, focusing the detection pattern of the array in a specific direction. The control station is realized by a ZedBoard which contains a Zynq-7000 system-on-chip. The actual beamforming algorithm is conducted in the FPGA portion of the Zynq-7000 system-on-chip. This allows for processing at low latency, a requirement for using the system in real-time. The control station also permits real-time playback to the user through either a hearing aid system or conventional headphones.

For testing and validation, a single microphone array was constructed using five high sensitivity MEMS microphones. Testing was conducted in a variety of locations around the Northeastern campus, including anechoic chambers, standard classrooms, and larger lecture halls. The results demonstrated the ability to target a specific desired speech source in a room. The degree of precision, and therefore the overall usefulness of the system, was a function of the number of microphone arrays, the number of microphones within those arrays, and the number of frequency sub-bands. Accommodation of these improvements could be accomplished through the use of a larger FPGA.

3 Problem Formulation

3.1 *Human Hearing*

The frequency range for healthy human hearing typically spans from 20 Hz to 20 kHz, with minimum sensitivity of 0 dB. Certain individuals with exceptional hearing may even be capable of hearing sounds as low as -15 dB. Unfortunately, the opposite scenario is far more common.

3.1.1 Hearing Loss

In order to understand hearing loss, one must first understand how the ear functions. When a sound enters the ear canal, a differential pressure is applied across a taut membrane known as the eardrum. An intricate network of small bones translates this motion to the cochlea, a fluid filled organ known for its characteristic nautilus shape. Pressure waves propagating through the fluid excite tiny hair-like nerves in the cochlea, producing an electrical signal which travels to the brain via bundles of nerves. Figure 1 shows the different regions of frequency sensitivity within the cochlea.

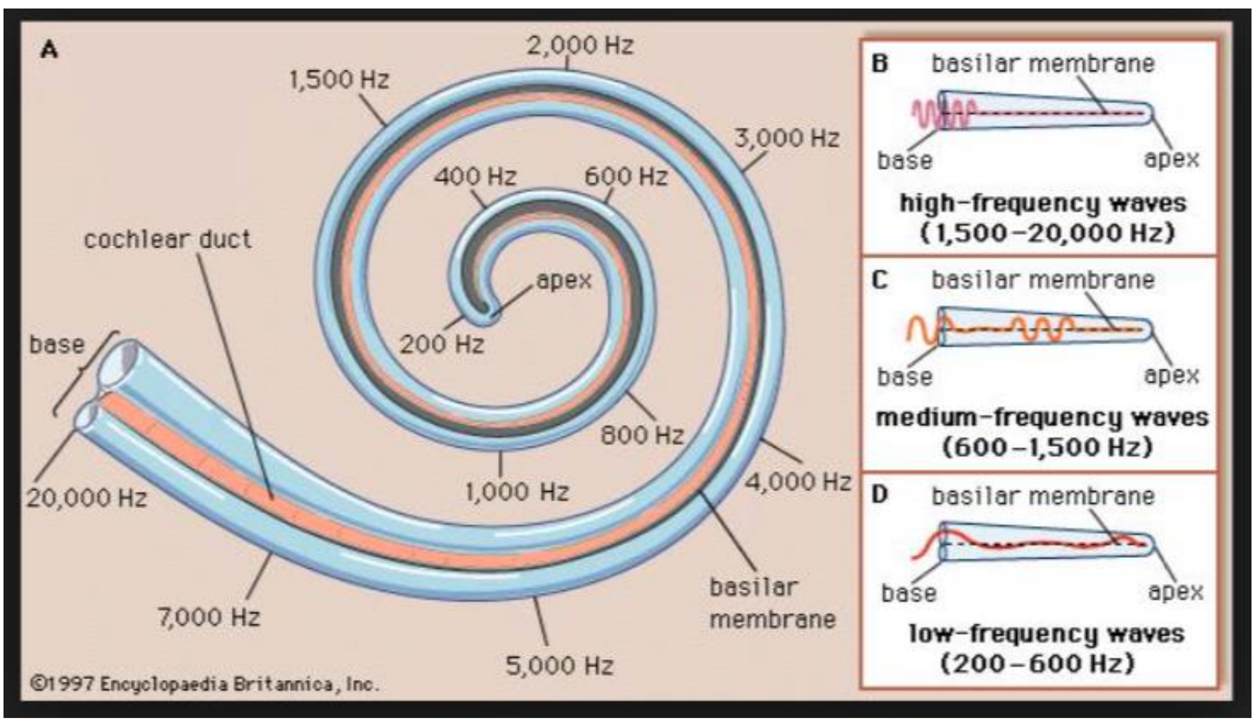

Figure 1: The cochlea [2]

The high-frequency sensitive nerves naturally tend to deteriorate with age. Premature damage to these nerves may also occur as a result of isolated events, including prolonged exposure to sounds over 85 dB, disease, developmental problems, or adverse reactions to medication.

4 Existing Solutions

Modern hearing aids are designed to improve speech intelligibility. In practice, however, hearing aids simply amplify all sounds indiscriminately [1]. This elicits a sensation of being closer to all sounds within the general vicinity. In the near-field, this solution typically accomplishes the stated objective of improved speech intelligibility. In the far-field, however, this solution is far less effective. This is due to a lack of microphone directionality and therefore a deterioration of signal to noise ratio.

5 Introduction

5.1 *Speech Perception*

Spoken language is composed of building blocks known as "phonemes." Phonemes include sounds like "th," "ch," and "sh." As shown in Figure 2, phonemes distributed as a function of frequency and loudness form a banana shape. As such, this distribution has been affectionately dubbed "the Speech Banana" [3].

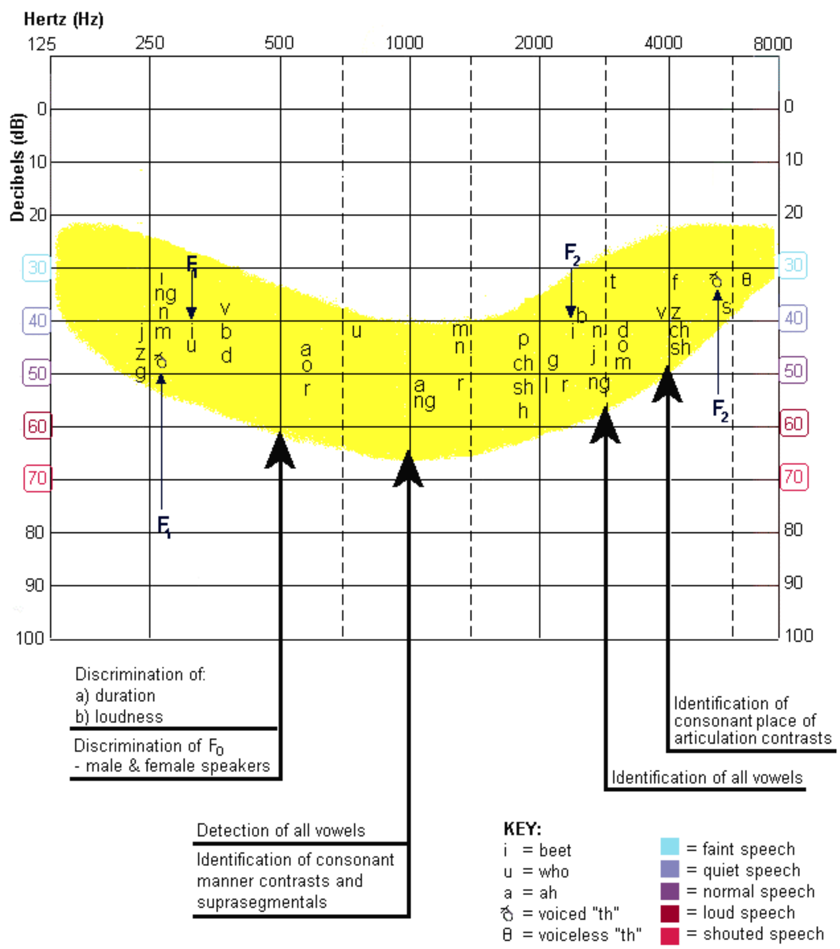

Figure 2: The Speech Banana [4]

Note that in general, vowel sounds occupy the lower-frequency end of the Speech Banana whereas consonant sounds occupy the higher-frequency end of the Speech Banana. Therefore, hearing-impaired individuals with compromised high-frequency sensitivity typically experience difficulty hearing consonant tones. This is detrimental to overall perception of speech.

5.2 *Microphone Arrays and Beamforming*

Acoustic beamforming is implemented using microphone arrays. As the name implies, microphone arrays are composed of microphones. Though there are many microphones available featuring non-uniform polar patterns, the discussion from this point forward will focus on arrays composed of omnidirectional microphones, as these types of microphones are most useful for array applications.

A microphone with an omnidirectional response receives sounds of all frequencies equally from all angles. This polar pattern is shown in Figure 3.

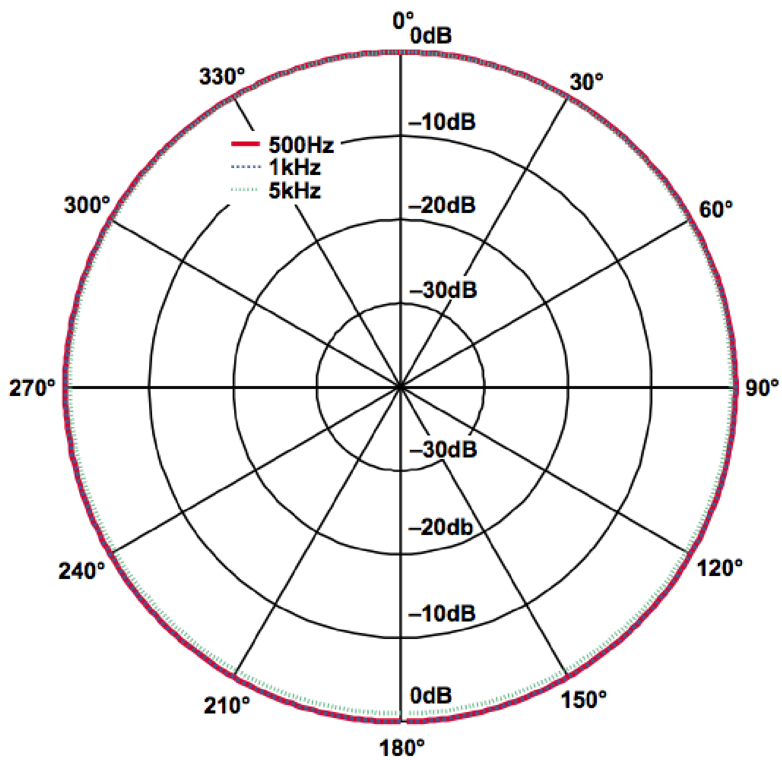

Figure 3: Polar pattern of an omnidirectional microphone [5]

When the outputs of multiple adjacent omnidirectional microphones are summed, their collective polar pattern deviates from this omnidirectional pattern. The exact directionality of the array is a function of geometry, frequency, and angle.

5.2.1 The Simplest Microphone Array

The simplest microphone array is composed of two microphones. This two-element, linear array can be configured as either a broadside or endfire array. When configured as a broadside array, as shown in Figure 4, the incoming signals from each microphone are simply summed together.

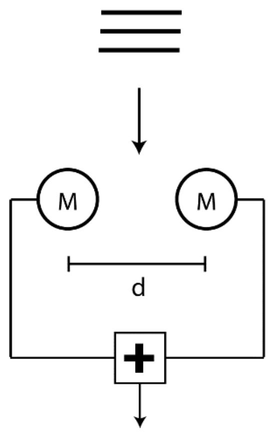

Figure 4: Microphone array in broadside configuration

Figure 5 shows the polar pattern of this configuration.

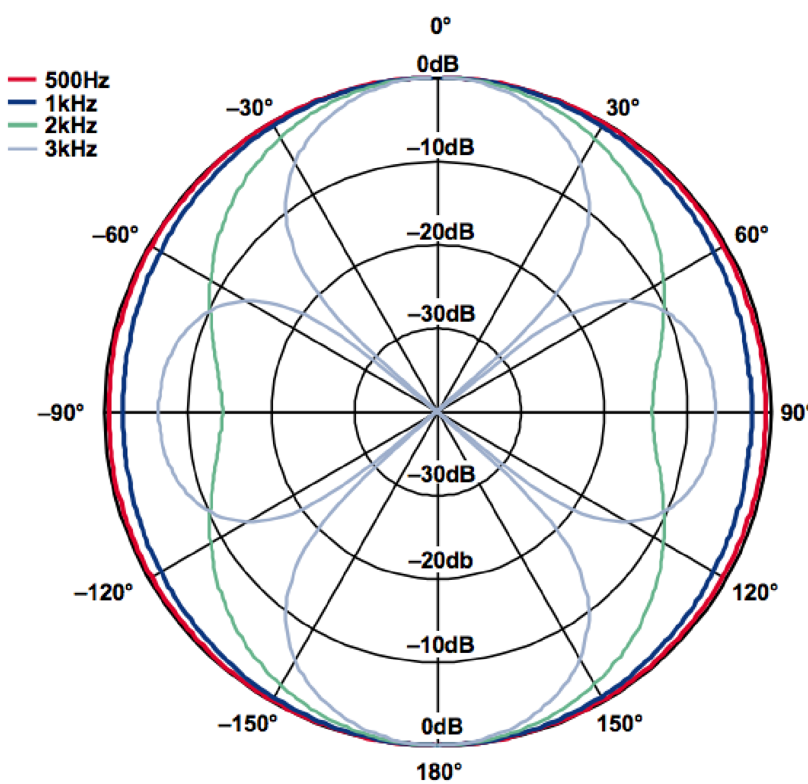

Figure 5: Polar pattern of a broadside array [5]

Note that the introduction of a second microphone has added directionality and frequency-dependence to the polar pattern of the array. As its name implies, a broadside array features a main lobe emanating from its broadside. That is, signals approaching the array at 0° from normal undergo zero attenuation. Due to the symmetric nature of the broadside array, a rear-facing lobe exists with magnitude equal to that of the main lobe. This rear-facing lobe is an inherent disadvantage of the broadside microphone array design.

The endfire array does not suffer from this disadvantage. An endfire array features a delay network prior to summation. This configuration is shown in Figure 6.

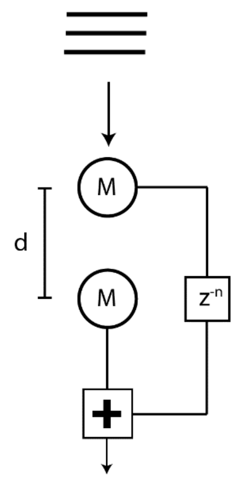

Figure 6: Microphone array in endfire configuration

The purpose of the delay network is to phase align the signals arriving at each microphone. The time delay is equal to the time needed for sound to travel distance *d*, given by equation 1

$$t = \frac{d}{c} \tag{1}$$

where *c* is the speed of sound. The sample delay *n* is given by equation 2

$$n = f_s t \tag{2}$$

where f_s is the sample rate of the system. Figure 7 shows the polar pattern of this configuration.

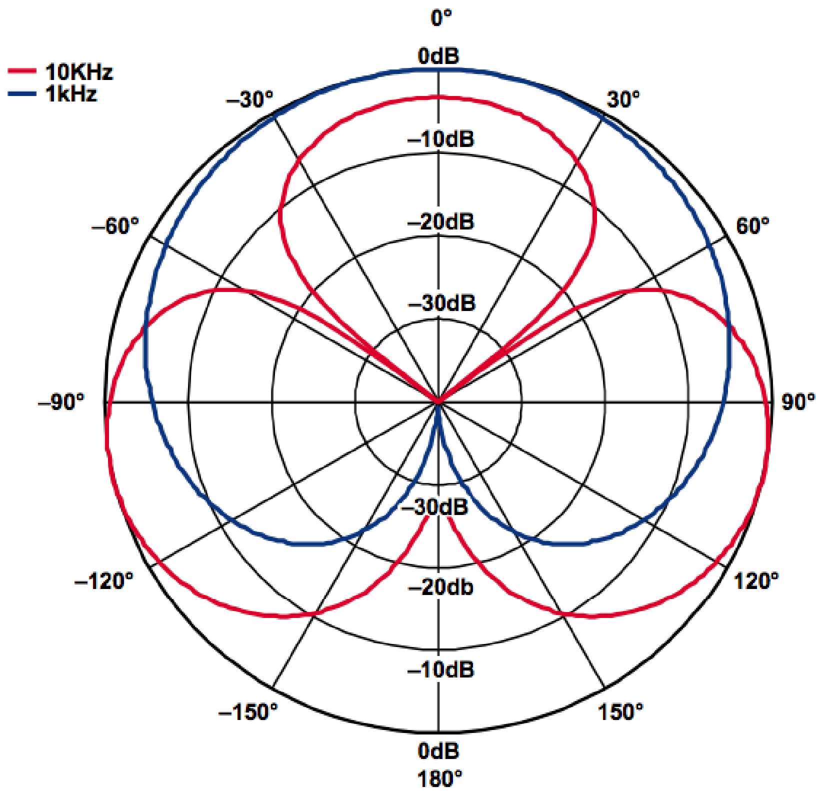

Figure 7: Polar pattern of an endfire array [5]

Note two important differences: (1) high attenuation in the direction opposite the main lobe for a wide band of frequencies (2) the main lobe of the endfire array resides in line with itself.

5.2.2 Beamforming

The two aforementioned microphone array designs are effective under the condition that the desired signals lie within the main lobe. In practice, however, desired signals may approach a microphone array from any direction.

Delay and sum beamforming addresses this problem. Delay and sum beamforming enables the virtual steering of the main lobe of a microphone array by varying the sample delay of the microphones closer to the desired signal. Delay and sum beamforming is extendible to a broadside microphone array of N microphones, as shown in Figure 8.

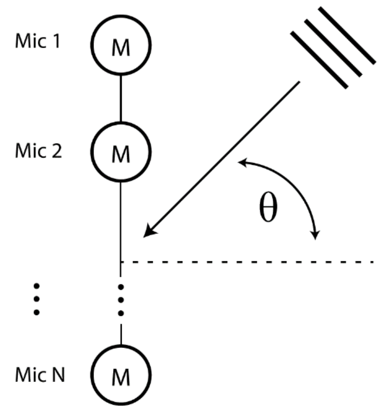

Figure 8: N element microphone array with signal incident at angle θ

Given an incoming plane wave of direction θ and frequency *f*, each microphone will receive a given wave front with a delay that is a function of its position in the array, the array spacing *d*, the angle θ, and the speed of sound *c*. This is given by equation 3.

$$\tau_n = \frac{(n-1)d\sin\theta}{c} \tag{3}$$

Note that the delay τ_n is zero for plane waves of normal incidence. For these plane waves, the collective output *y(t)* of the microphone array is given by equation 4

$$y(t) = \frac{1}{N}\sum_{n=1}^{N} x_n(t) \tag{4}$$

where $x_n(t)$ is the signal seen by each microphone. Delay and sum beamforming is implemented by multiplying the spectral content of signals arriving at each microphone by complex weights which are a function of delay τ_n. This is given by equation 5.

$$W_n(f,\theta) = \frac{1}{N}e^{-j2\pi f\tau_n} \tag{5}$$

Note that θ now represents the desired steering angle. The resulting frequency-dependent signal is given by equation 6.

$$y(f,\theta) = \frac{1}{N}\sum_{n=1}^{N} x(f,\theta)w_n(f,\theta) \tag{6}$$

The resulting time-dependent signal is given by equation 7.

$$y(t) = \frac{1}{N}\sum_{n=1}^{N} x(t - \tau_n) \tag{7}$$

Figure 9 shows the capability of delay and sum beamforming. The polar pattern on the left is that of a non-steered three-element microphone array. The polar pattern on the right is that of the same microphone array steered at an angle of 30°.

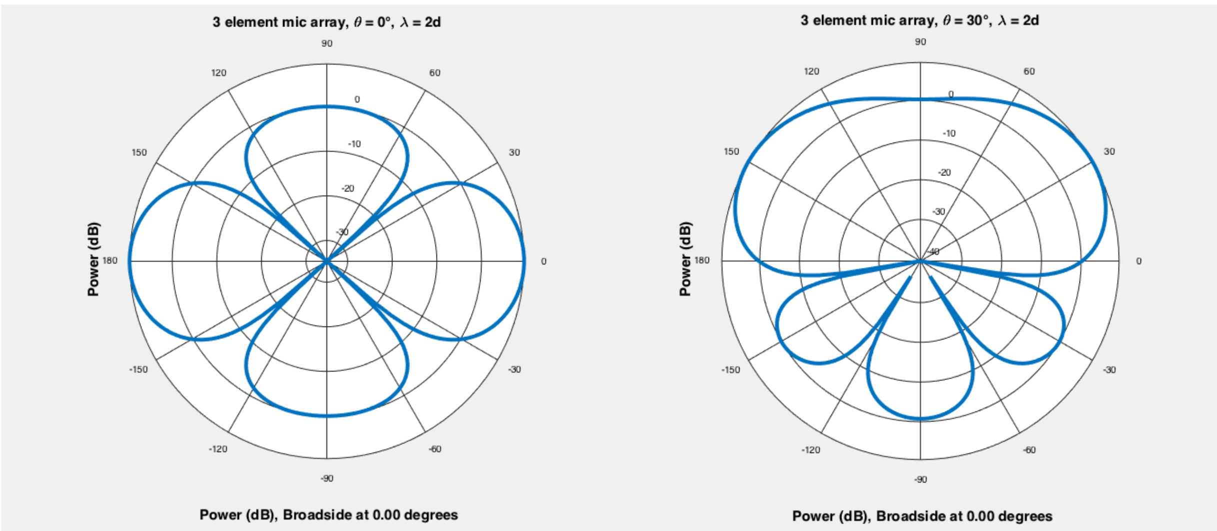

Figure 9: Capability of delay and sum beamforming

For a microphone array of fixed spacing *d*, the polar response is ideal for incoming waves of wavelength $\lambda = 2d$. This corresponds to the center frequency of the microphone array. If the wavelength λ deviates larger, the main lobe of the polar response grows wider and therefore less directional. If the wavelength λ deviates smaller, the main lobe of the polar response grows narrower and therefore more directional, but at the expense of spatial aliasing. Spatial aliasing manifests itself as grading lobes, or off-axis lobes equal in magnitude with the main lobe. Figure 10 shows the effects of wideband use of a microphone array of fixed spacing. The polar pattern on the left is that of a three-element microphone array subject to waves of wavelength $\lambda = 5.04d$. The polar pattern on the right is that of the same microphone array subject to waves of wavelength $\lambda = 1.26d$. Note that the side lobes are transitioning into grating lobes.

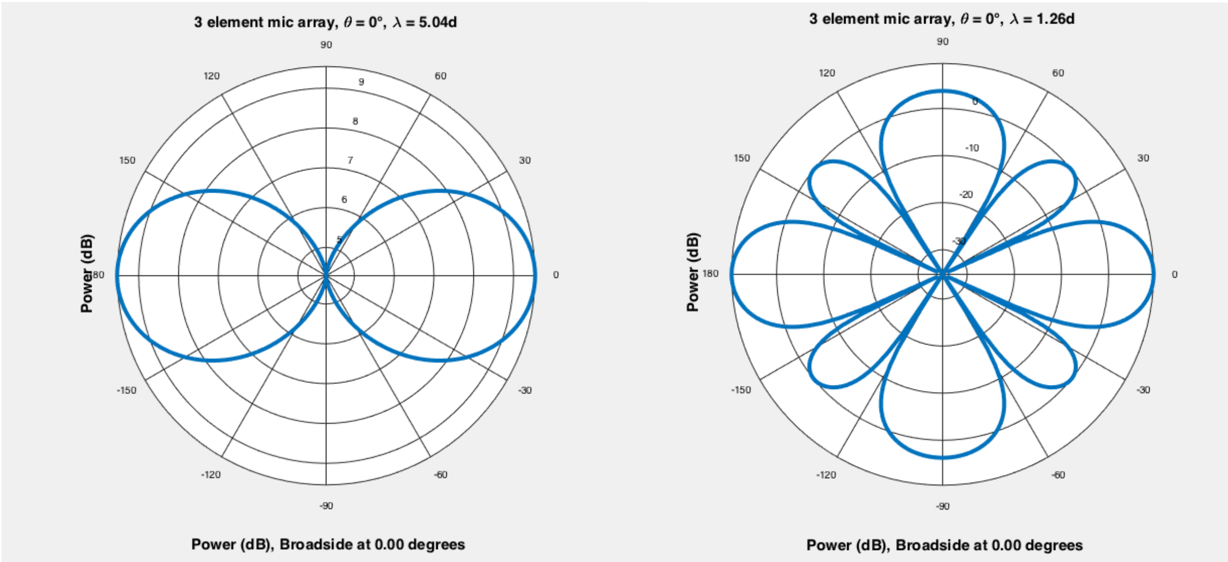

Figure 10: Wideband use of a fixed-spacing microphone array

6 Implementation

Having demonstrated the efficacy of the design using simulations, the SoundSelect Array System team developed a prototype system featuring a single microphone array. Figure 11 shows the concept for the prototype system.

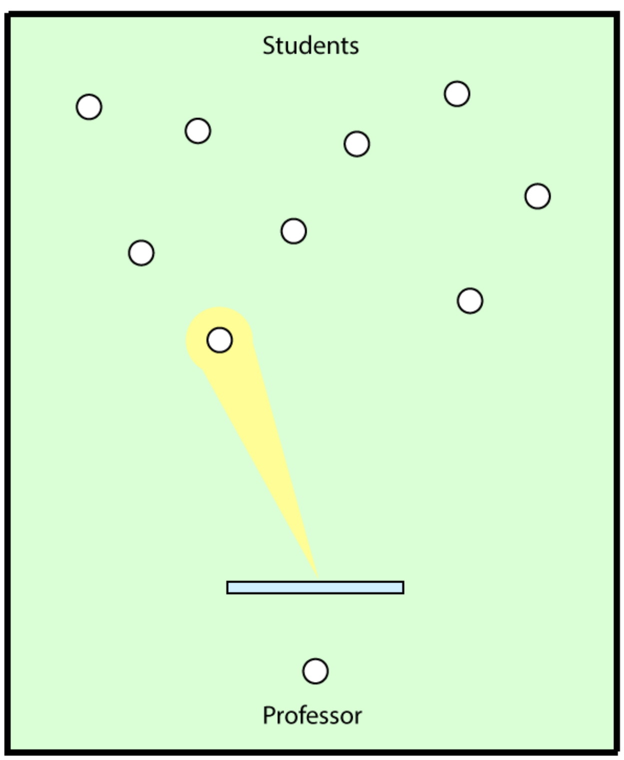

Figure 11: Prototype system concept

The prototype system is tailored for operation in a typical classroom, with professor occupying the front of the room and students occupying the remaining space. The microphone array and control station are placed at the front of the room within arm's reach of the professor. By operating a series of switches on the control station, the professor can select the direction of desired listening.

6.1 *System Level Design*

Figure 12 shows the block diagram of the prototype system.

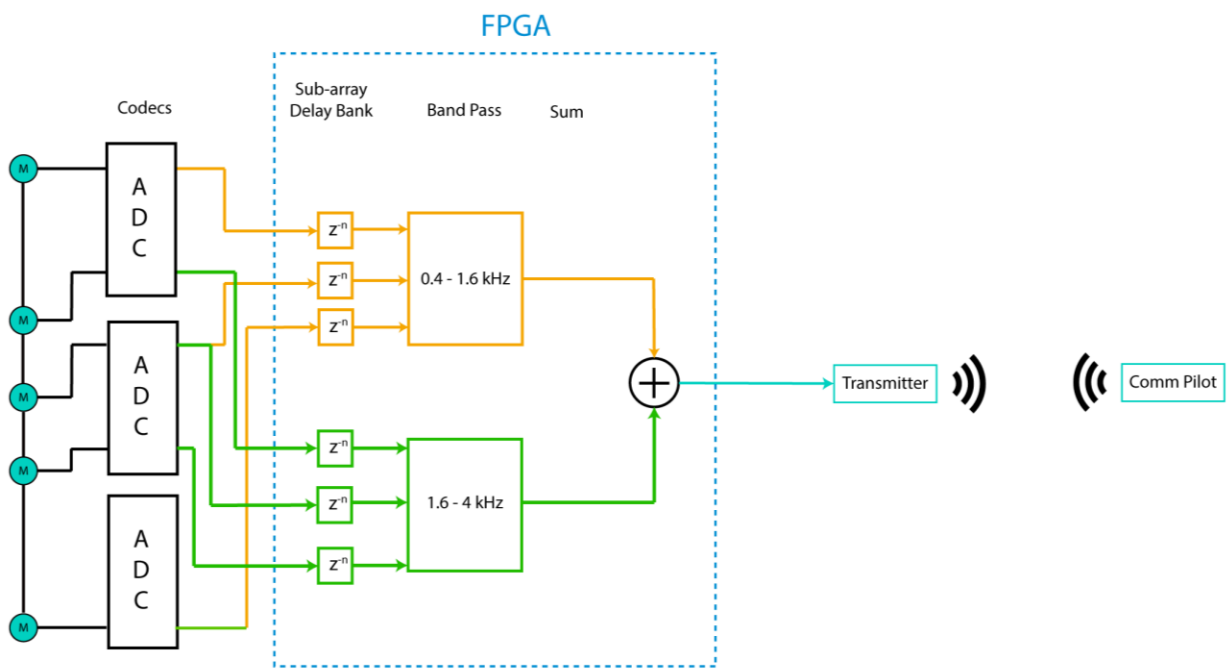

Figure 12: Prototype system block diagram

System flow begins in real-time with the individual microphones shown on the left (cyan). Together, these microphones compose the complete array. Analog audio signals travel from each microphone to the ADC inputs of the audio codecs. The audio codecs then transmit digital audio signals to the FPGA using the I^2S protocol. Within the FPGA, beamforming is conducted by the delay banks; each sub-array of the composite array undergoes separate beamforming operations. The timing weights used within the delay banks are governed by the selected angle. The respective signals from each sub-array are then sent to bandpass filters, summed, and transmitted to the user.

6.2 *Composite Microphone Arrays*

The SoundSelect Array System features a composite microphone array. A composite microphone array is a microphone array of variable-spacing created by overlapping sub-arrays of fixed-spacing. Figure 13 shows the composite microphone array used by the SoundSelect

Array System. This implemented composite microphone array (cyan) is the result of nesting a three-element microphone array of 6.1 cm spacing (green) within a three-element microphone array of 17 cm spacing (orange). The larger sub-array features a center frequency of 1 kHz and a bandwidth of 1.2 kHz. The smaller sub-array features a center frequency of 2.8 kHz and a bandwidth of 2.4 kHz. Note that the center microphone of the two sub-arrays is shared within the composite array.

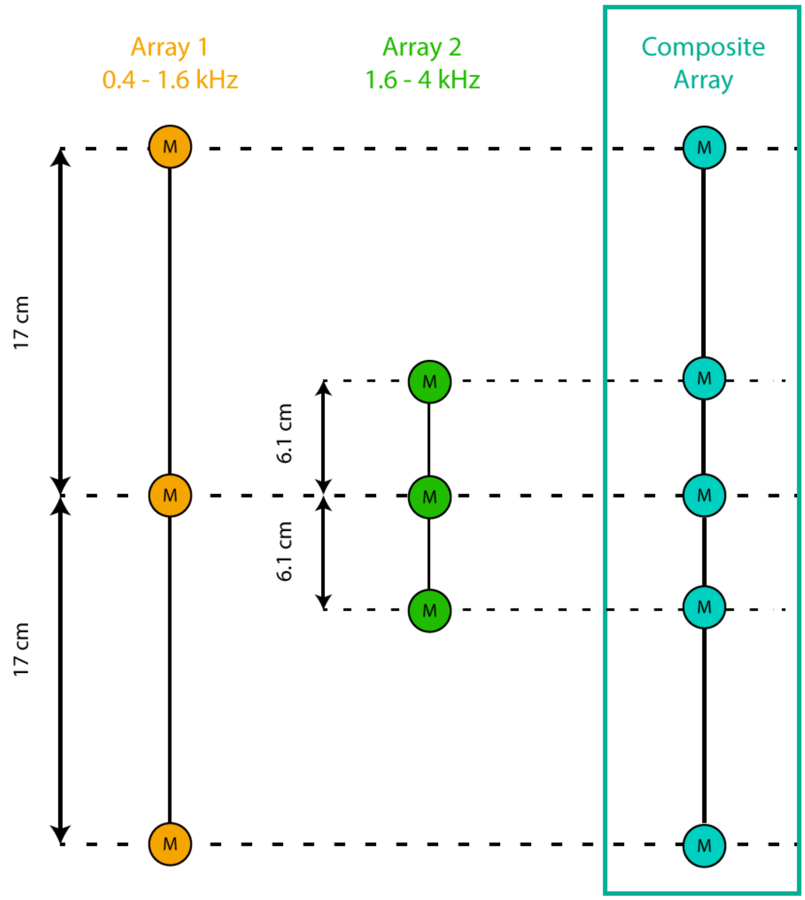

Figure 13: Composite microphone array

The motivation for such a design is to support an acceptable level of performance across a wide band of frequencies. By distributing the responsibility of servicing a wide band of frequencies across multiple microphone arrays, the average deviation from the center frequency of a given microphone array is limited.

6.3 *Audio Frequency Filtering*

The composite microphone array relies on the ability to limit the use of the sub-arrays exclusively to the portions of the speech band for which they were optimized. This ability is realized by FIR bandpass filtering. FIR filtering presents two main advantages over traditional IIR filtering: (1) linear phase response yields constant group delay across the entire passband and therefore perfect signal alignment prior to summation. This is necessary to prevent audio distortion (2) lack of feedback prevents accumulation of fixed-point rounding error. Figure 14 shows the magnitude responses of the 96 order FIR bandpass filters used by the SoundSelect Array System. Band 1 (blue), corresponding to the larger sub-array, has -6 dB cutoff frequencies at 0.4 and 1.6 kHz. Band 2 (red), corresponding to the smaller sub-array, has -6 dB cutoff frequencies at 1.6 kHz and 4 kHz.

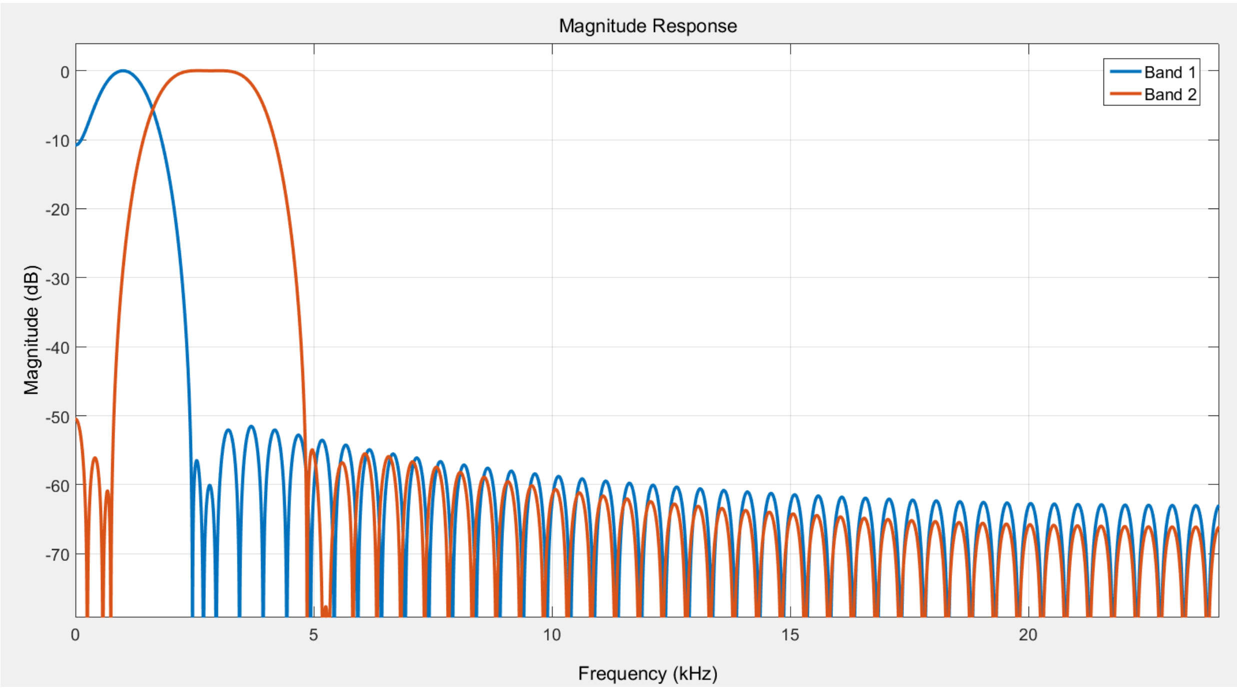

Figure 14: Real-time FIR filtering magnitude responses

Note that the filters contribute only 1 ms of latency to the algorithm as a whole. This is well below the level of human perception.

6.4 *Hardware Specification*

6.4.1 Processing

The SoundSelect Array System requires massively parallel synchronous operations to be executed with a level of timeliness not achievable in a standard microcontroller. For this reason, the prototype system was realized with an FPGA-based solution. The ZedBoard development kit met all design requirements while also providing several additional luxuries.

The ZedBoard features a Xilinx Zynq-7000 system-on-chip which includes both an FPGA and an ARM processor. The FPGA meets the latency requirements of the digital signal processing while the ARM processor handles the audio codec boot-up configuration. The ZedBoard package also features GPIO including buttons, switches, and LEDs. These were necessary for control of the system.

6.4.2 Microphones

The composite array used by the SoundSelect Array System is composed of analog MEMS microphones. The analog aspect of the microphones provides two main advantages: (1) ability to transmit signals over long distances (2) ease of integration with audio codecs. The MEMS aspect of the microphones provides two main advantages: (1) high far-field sensitivity (2) small physical package. Each microphone is powered by a regulated 3.3 VDC power supply. A sample MEMS microphone is shown in Figure 15.

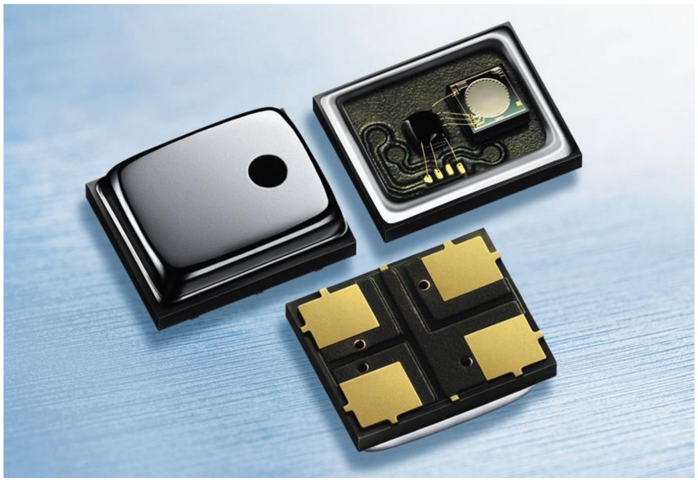

Figure 15: Sample MEMS microphone

6.4.3 Audio Codecs

The MEMS microphones interface with the FPGA through Analog Devices ADAU1761 audio codecs. The block diagram of the ADAU1761 is shown in Figure 16.

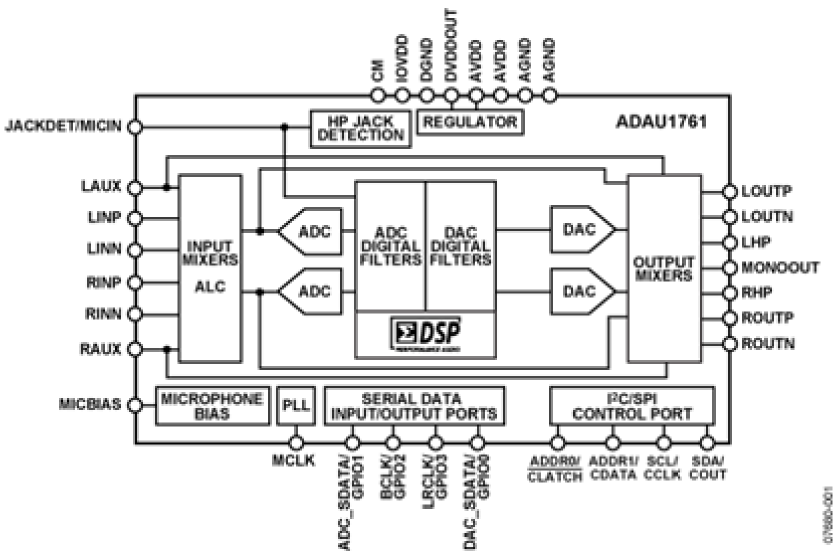

Figure 16: Audio codec block diagram

The ADAU1761 supports many resolutions and sampling rates which are programmable via an I^2C interface. The SoundSelect Array System operates the audio codecs at a 24-bit resolution and 48 kHz sampling rate. This sampling rate is more than adequate for the system's highest frequency of interest, 4 kHz.

Audio information is transmitted to the FPGA using the I^2S protocol. Figure 17 shows the I^2S protocol.

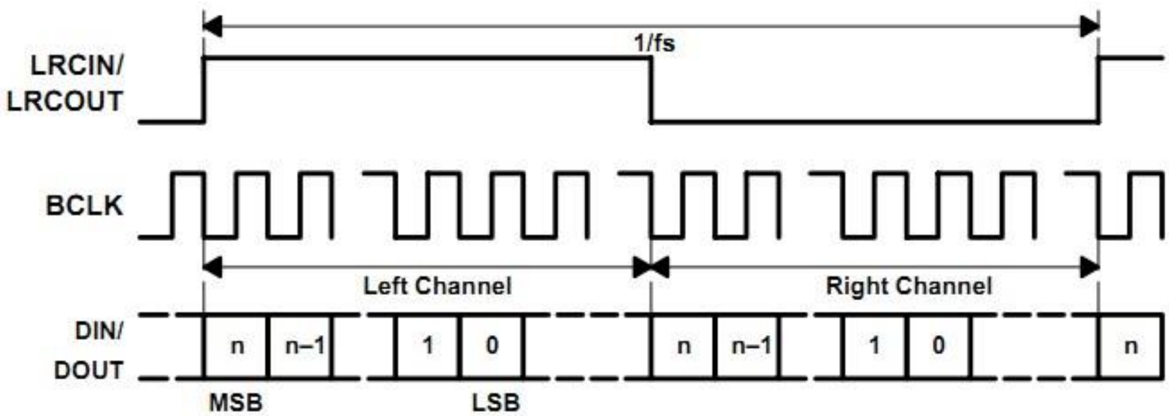

Figure 17: I^2S protocol [6]

The I^2S protocol is composed of three signals: LRCOUT, BCLK, and DOUT. LRCOUT indicates which audio channel, left or right, is being transmitted. When LRCOUT is high, the left channel is being transmitted. When LRCOUT is low, the right channel is being transmitted. BCLK synchronizes the transmission of audio information, which is carried out on DOUT.

7 Testing

7.1 *Test Description*

The SoundSelect Array System was tested in a typical classroom of width 8 meters and depth 10 meters. The microphone array and control station were placed along the center of the front wall, simulating a professor in front of a classroom of students. With the microphone array steered at angle of 38.5° from broadside, a speech sample was played and recorded from nine different positions within the room. The power of each recorded speech sample was calculated, normalized, and compared to simulated results.

7.2 *Test Results*

Figure 18 shows a comparison of the simulated and observed test results. The image on the left shows the simulated attenuation pattern within an ideal room (i.e. a room with non-reflective walls and no signal attenuation as a function of distance travelled). Warm colors represent physical regions of low attenuation. Cool colors represent physical regions of high attenuation, with the coolest shade of indigo saturating at -8 dB. The image on the right shows the observed attenuation pattern within the room quantized according to the location and power of each recorded speech sample.

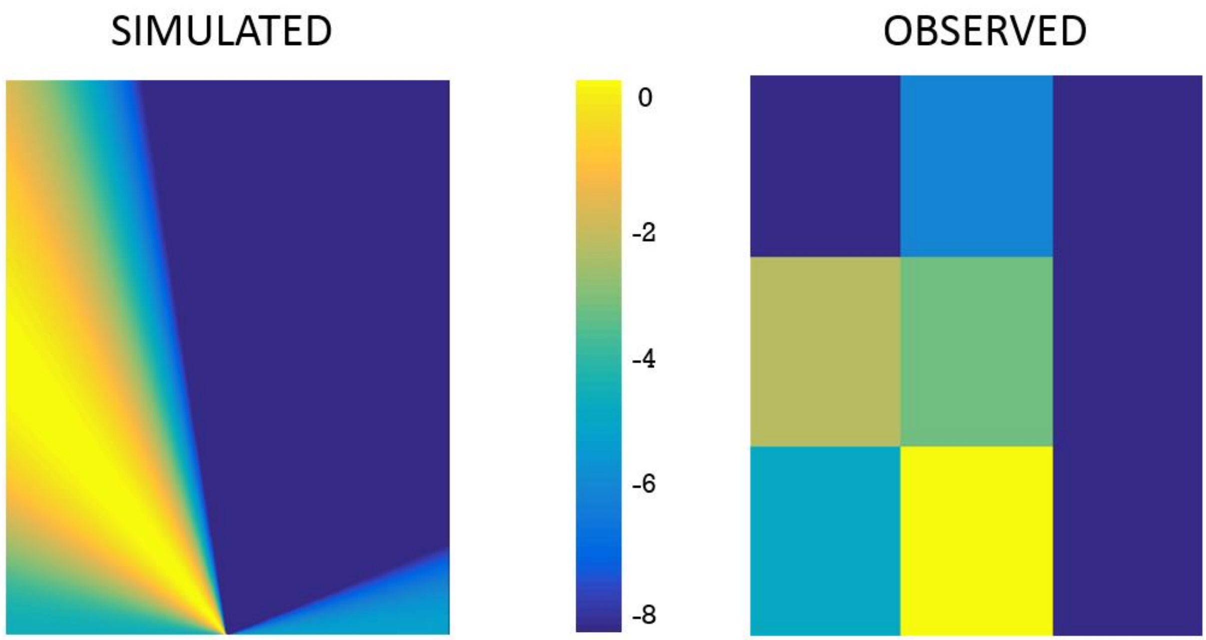

Figure 18: Simulated vs observed results

Note that the warmest region within the observed attenuation pattern falls directly in front of the microphone array. This is because sounds from this region have the least distance to travel to the microphone array, and therefore undergo the least attenuation as a function of distance travelled. The second warmest region falls directly in line with the steering vector. The coolest region of the room, the rightmost third, is consistent with the simulation. Note that the slight warmth of the uppermost central region is a result of reflections off the leftmost wall and along the steering vector.

8 System Enhancements

The design of the prototype SoundSelect Array System was most limited by the number of logic cells within the FPGA portion of the Zynq-7000 system-on-chip. Having a larger FPGA would permit the addition of a second microphone array, thereby extending the directional isolation of the existing prototype to point isolation. The SoundSelect Array System team has coined this advanced beamforming technique as "spotlight" beamforming. Figure 19 shows the concept for the next generation system.

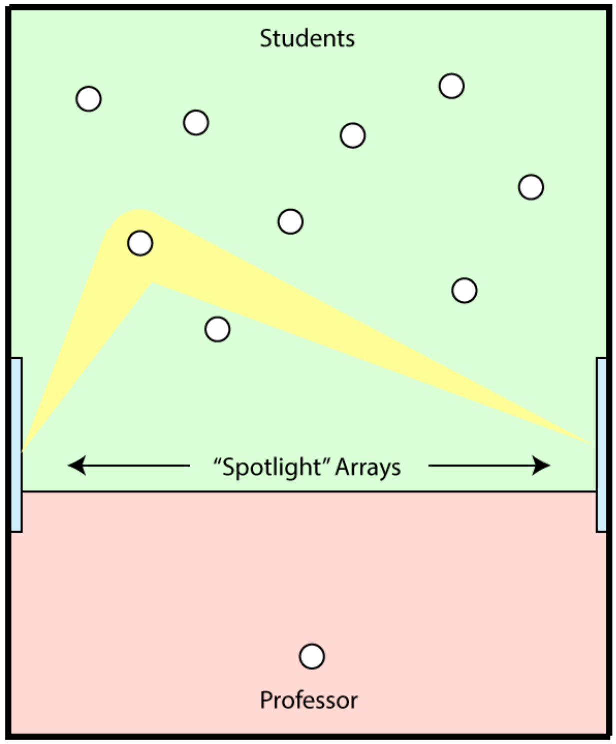

Figure 19: Next generation system concept

Like the prototype system, the next generation system is tailored for operation in a typical classroom. The control station remains at the front of the room within arm's reach of the professor. However, the microphone arrays now lay flush on the opposing walls of the room. The spotlight array configuration features an increased immunity to the effects of reverberation, as flushness against the walls limits reception of early reflections.

8.1 *Expected Performance*

Figure 20 shows the block diagram of the next generation system.

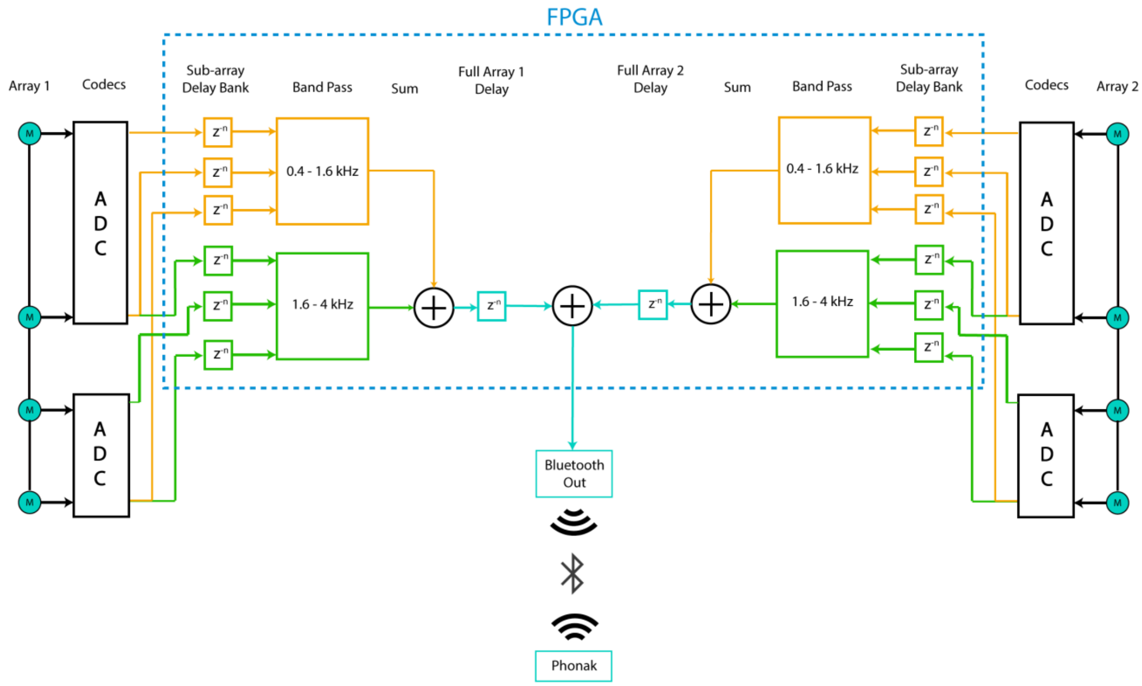

Figure 20: Next generation system block diagram

System flow begins in real-time with the individual microphones shown on the left and right (cyan). Together, these microphones compose the two complete arrays. Note that the next generation microphone arrays are asymmetrical with four microphones instead of five. This is because in the next generation system, each array is only responsible for a 90° section of the room, permitting the removal of the fifth microphone at no cost to performance. As before, analog audio signals travel from each microphone to the ADC inputs of the audio codecs. The audio codecs then transmit digital audio signals to the FPGA using the I^2S format. Within the FPGA, beamforming is conducted by the delay banks; each composite array as well as each sub-array with said composite arrays undergoes separate beamforming operations. The timing weights used within the delay banks are governed by the selected position. The respective signals from each sub-array within a given composite array are then sent to bandpass filters and summed. The two remaining signals from the two respective composite arrays then travel through a delay compensation network to ensure phase alignment prior to final summation. Once summed, the final signal is transmitted to the user via Bluetooth connection.

8.2 *Predicted Performance*

Figure 21 shows the simulated attenuation pattern of the next generation system.

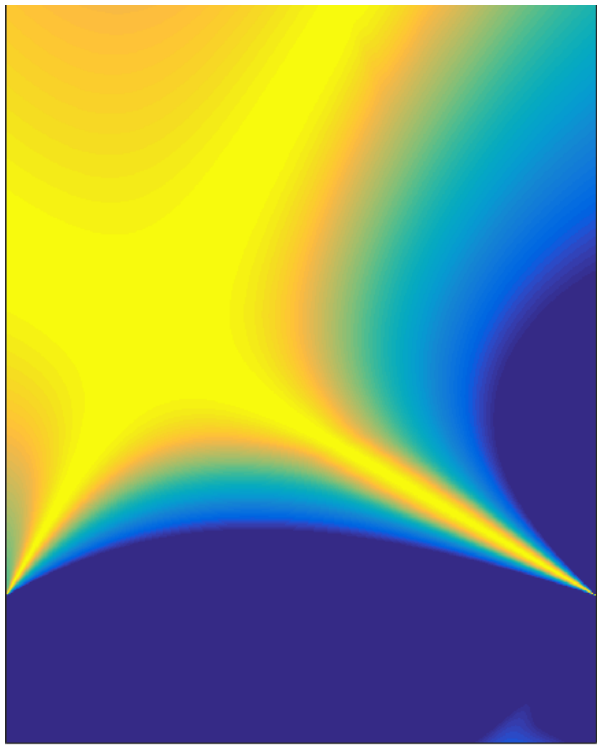

Figure 20: Next generation system simulated attenuation pattern

Point isolation can be rendered sharper given other enhancements, including additional sub-arrays, additional microphones per sub-array, and higher order bandpass filters. The benefit of additional microphones per sub-array, for example, is shown in Figure 21. The leftmost attenuation pattern is one of a system featuring four microphones per sub-array. The middle attenuation pattern is one of a system featuring five microphones per sub-array. The rightmost attenuation pattern is one of a system featuring seven microphones per sub-array.

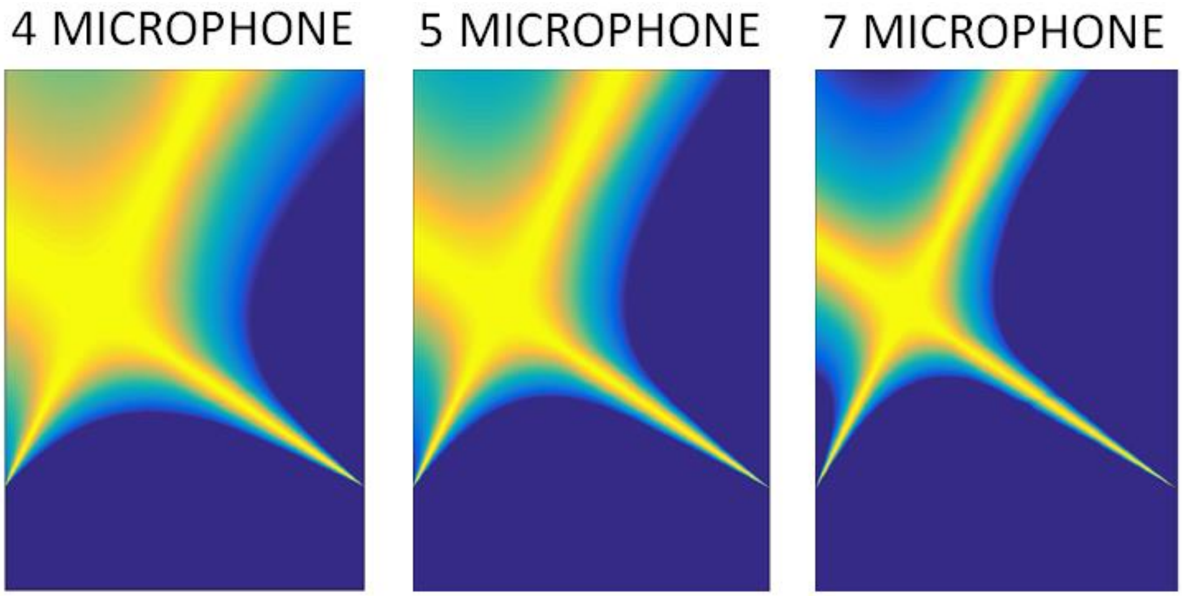

Figure 21: Benefit of additional microphones per sub-array

Note that the attenuation pattern grows sharper with additional microphones in each sub-array.

9 References

[1] N. Disarno, "What should be Done About Hearing Loss?" *The New York Times*, Feb. 27, 2013. [Online]. Available: http://www.nytimes.com. [Accessed Aug. 16, 2015].

[2] "Electrodes and Channels," *Cochlear Implant HELP.* [Online]. Available: http://cochlearimplanthelp.com/journey/choosing-a-cochlear-implant/electrodes-and-channels/. [Accessed: Aug. 16, 2015]

[3] "The Speech Banana," *Listening and Spoken Language Knowledge Center.* [Online]. Available: http://www.listeningandspokenlanguage.org/SpeechBanana/. [Accessed: Aug. 16, 2015]

[4] "Speech Banana: Interpretation of Acoustics of Speech," *First Years Development Through Distance Education.* [Online]. Available: http://firstyears.org/c1/u2/banacoustics.htm. [Accessed: Aug. 19, 2015]

[5] "Microphone Array Beamforming," *InvenSense.* Dec. 31, 2013. [Online]. Available: http://www.invensense.com/wp-content/uploads/2015/02/Microphone-Array-Beamforming.pdf. [Accessed: Aug. 20, 2015].

[6] "TLV320AIC23B Data Manual," *Texas Instruments*, February 1' 2004. [Online]. Available: http://www.ti.com/lit/ds/symlink/tlv320aic23b.pdf. [Accessed: December 17, 2015].

10 Appendix

10.1 *Prototype Microphone*

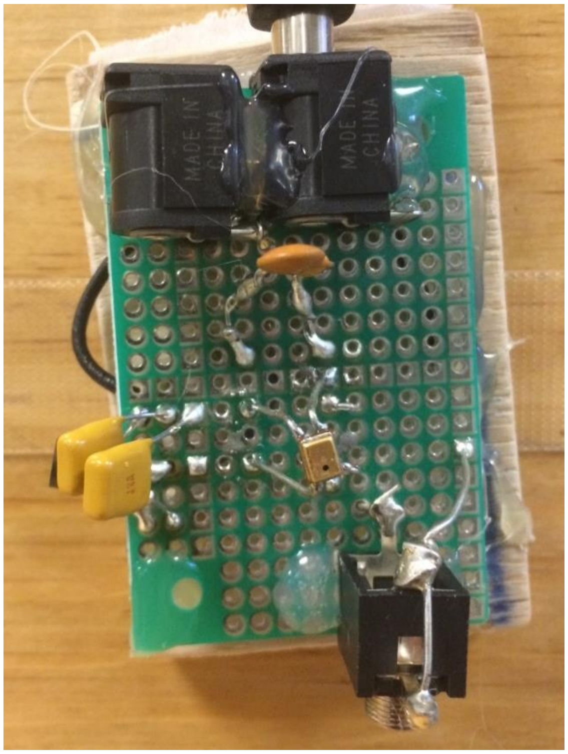

10.2 *Prototype Microphone Array*

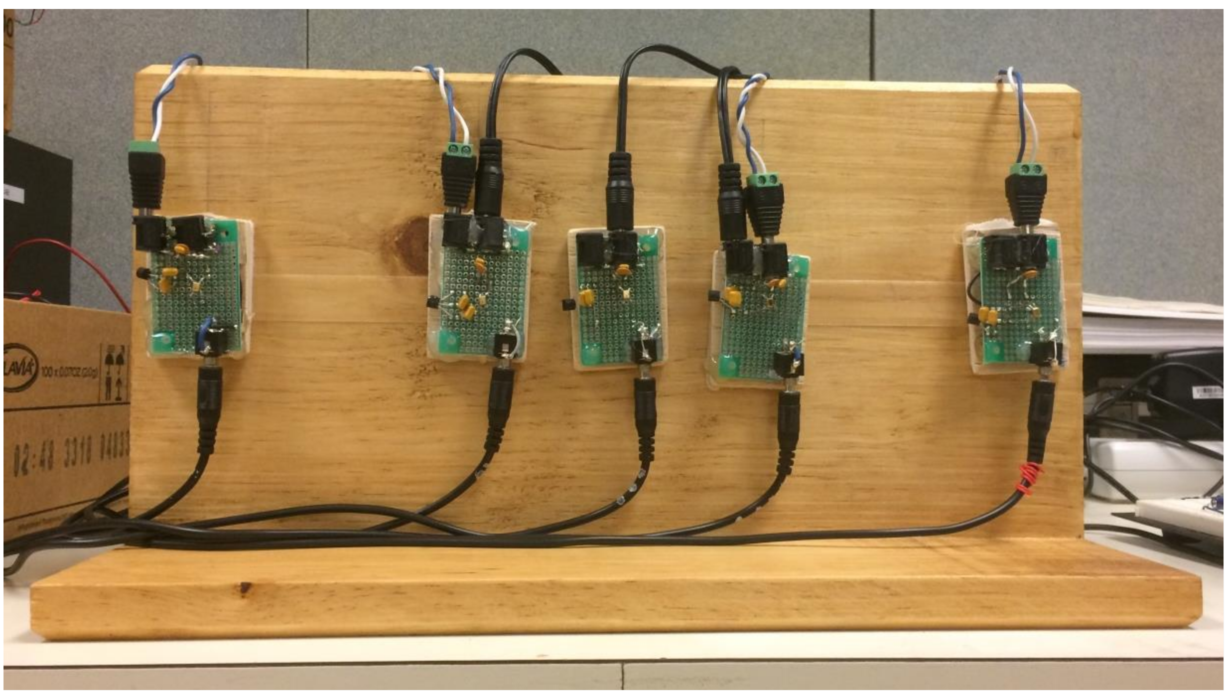

10.3 ***Prototype Control Station***

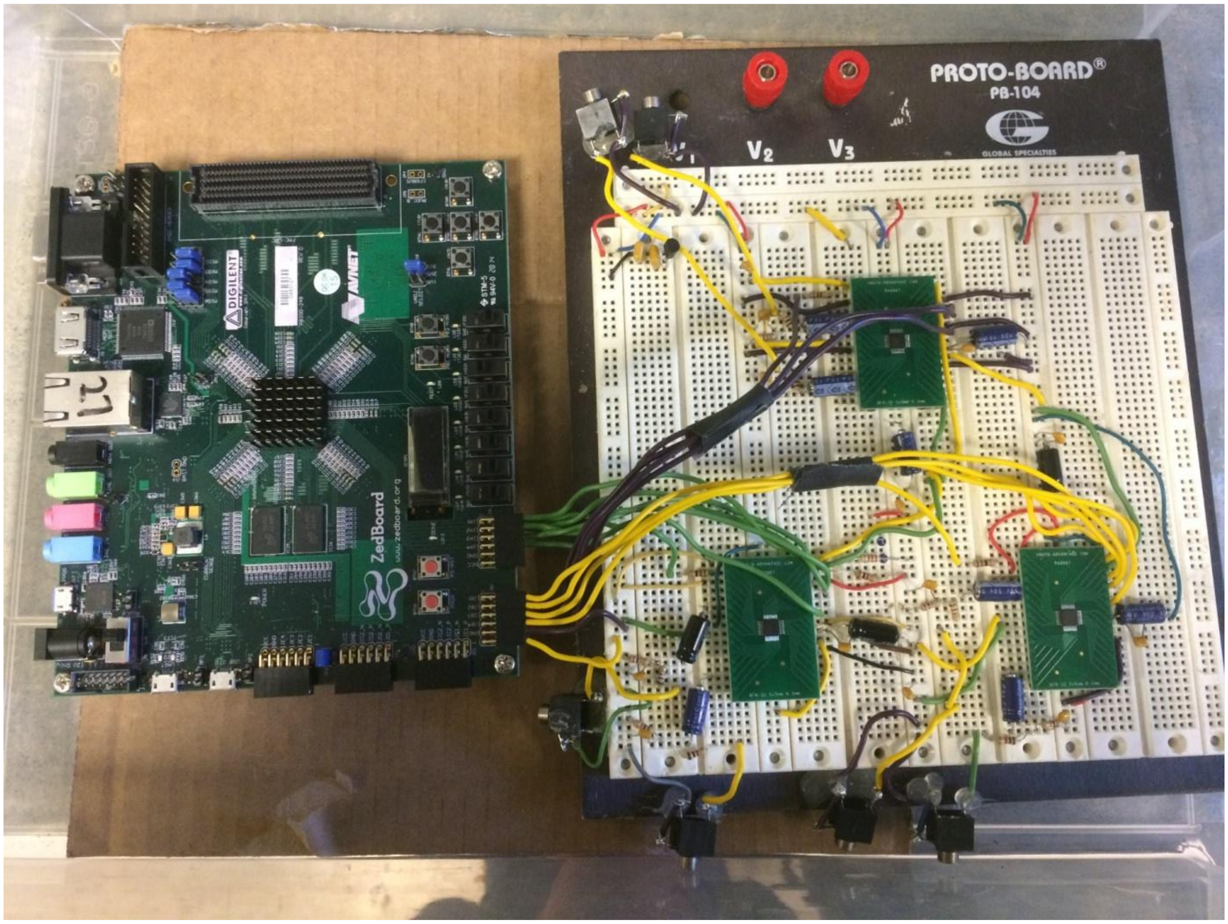

10.4 ***Prototype System***

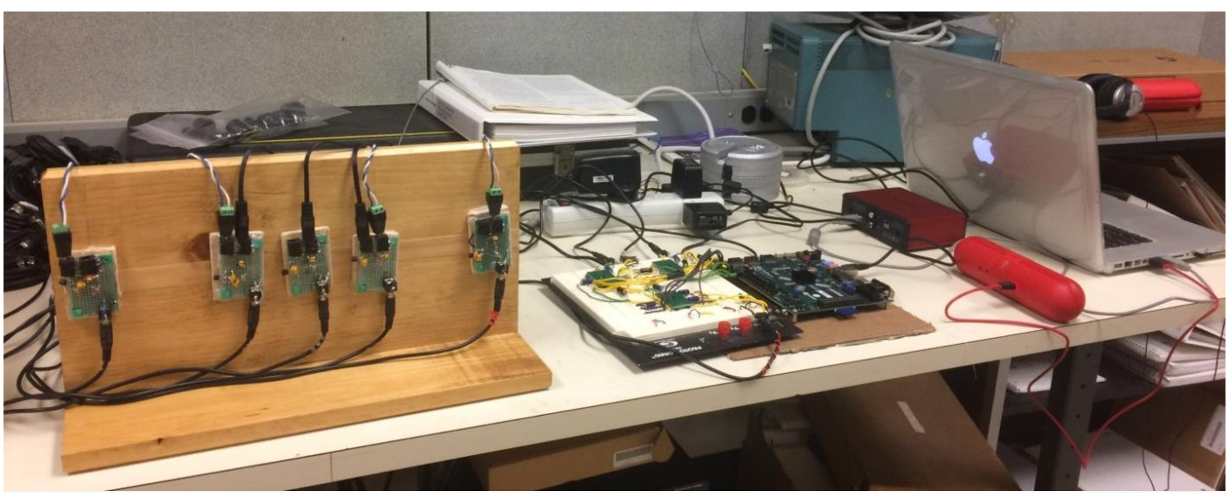

10.5 ***Prototype Bill of Materials***

Retailer	Part Number	Item	Item Cost	Quantity	Total Cost
Mouser Electronics	SPU0414H5RH-SB	Knowles MEMS Microphones	$1.01	5	$5.05
Amazon.com	AUD-1100-25-2PK	Cables Unlimited AUD-1100-25-2PK (Pack of 2) 3.5 mm 25ft cable	$7.00	5	$35.00
Proto Advantage	ADAU1761BCPZ-ND	Analog Devices Audio Codec, Adapter, & Assembly	$34.04	3	$102.12
Amazon.com	002-9493862-4216232	Pack of 30 Prototype Perfboard 2"x1.34" 250hole Epoxy Fiber Pitch 0.1"	$10.84	1	$10.84
DigiKey	62-1165-ND	AC/DC WALL MOUNT ADAPTER 3.3V 5W	$8.76	3	$26.28
DigiKey	CP-037A-ND	CON PWR JCK 2.0 X 6.5MM W/O SW	$0.63	10	$6.34
DigiKey	CP-3536NG-ND	CONN AUDIO JACK 3.5MM MONO	$0.85	10	$8.50
DigiKey	MCP1700-3302E/TO-ND	IC REG LDO 3.3V 0.25A TO92-3	$0.31	25	$7.75
Amazon.com	113-6756323-0456248	Omall 20 pair2.1x5.5mm Jack DC Power Adapter	$15.99	1	$15.99
Amazon.com	113-2841404-2333855	VELCRO - Sticky Back - 15' x 3/4" Tape - Clear	$15.73	1	$15.73
Digilent	ZEDBOARD	ZedBoard - Education Edition	$319.00	1	$319.00
				TOTAL:	**$552.60**

10.6 *Total Project Expenses*

Retailer	Order Number	Order Date	Item	Item Cost	Quantity	Shipping	Total Cost
Adafruit	871687	9/9/2015	SMT Breakout PCB for SOIC-28 - 3 Pack	$4.95	4	$7.01	$26.81
Digilent	2015-213102	9/9/2015	PMOD-CABLEKIT-6PIN	$3.99	6	$11.09	$35.03
Mouser Electronics	9246598	9/10/2015	Kycon Phone Connectors	$1.11	25	$6.99	$34.74
Mouser Electronics	9246598	9/10/2015	TI Interface - CODECs	$7.12	10	$0.00	$71.20
Mouser Electronics	9246598	9/10/2015	Knowles MEMS Microphones	$1.01	50	$0.00	$50.50
Mouser Electronics	9264182	9/14/2015	TI WiFi / 802.11 Development Tools	$39.79	1	$4.99	$44.78
AVNET	5527054	9/14/2015	WiLink 8 Wi-Fi and BT/BLE Pmod Adaptor	$34.00	1	$8.00	$42.00
Amazon.com	113-9217130-8545048	9/17/2015	Monoprice Fastening Tape 0.75inch One Wrap Hook & Loop	$6.39	2	$0.00	$12.78
Amazon.com	109-8283161-6233037	10/2/2015	Cables Unlimited AUD-1100-25-2PK (Pack of 2) 3.5 mm 25ft cable	$7.00	5	$0.00	$35.00
Proto Advantage	22764	10/5/2015	LFCSP-32 to DIP-32 SMT Adapter & Assembly	$19.39	7	$4.00	$139.73
Proto Advantage	22764	10/5/2015	Analog Devices Audio Codec: ADAU1761BCPZ-ND	$14.65	7	$0.00	$102.55
Amazon.com	002-9493862-4216232	10/7/2015	MG Chemicals 4860P-35G Solder Paste, Sn63/Pb37, No Clean	$15.69	1	$0.00	$15.69
Amazon.com	002-9493862-4216232	10/7/2015	Pack of 30 Prototype Perfboard 2"x1.34" 250hole Epoxy Fiber Pitch 0.1"	$10.84	1	$0.00	$10.84
Amazon.com	002-9493862-4216232	10/7/2015	Elenco Electronics TL-21 Minigrabber to Minigrabber 5 pc Test Lead Set	$8.90	1	$0.00	$8.90
DigiKey	44500334	10/19/2015	AC/DC WALL MOUNT ADAPTER 3.3V 5W	$8.76	3	$21.01	$47.29
DigiKey	44500334	10/19/2015	CON PWR JCK 2.0 X 6.5MM W/O SW	$0.63	30	$0.00	$19.02
DigiKey	44500334	10/19/2015	CONN AUDIO JACK 3.5MM MONO	$0.85	10	$0.00	$8.50
DigiKey	44500334	10/19/2015	IC REG LDO 3.3V 0.25A TO92-3	$0.31	25	$0.00	$7.75
Amazon.com	113-6756323-0456248	10/30/2015	Xuron 170-II Micro-Shear Flush Cutter	$8.80	1	$0.00	$8.80
Amazon.com	113-6756323-0456248	10/30/2015	Omall 20 pair2.1x5.5mm Jack DC Power Adapter	$15.99	1	$0.00	$15.99
Amazon.com	113-6756323-0456248	10/30/2015	2 Nail Art Tweezers Curved Straight Pointed Ongles (silver) (silver)	$4.58	1	$0.00	$4.58
Amazon.com	113-2841404-2333855	11/6/2015	VELCRO - Sticky Back - 15' x 3/4" Tape - Clear	$15.73	1	$0.00	$15.73
RadioShack	44292	11/23/2015	3VDC/700MA ACDC Converter	$6.97	4	$0.00	$27.88
					TOTAL:		**$786.09**
		Notes:					
		***Shipping costs, if any, are included with the first item from each order**					